SWIRLING FLOW IN ROUGH CONICAL DIFFUSERS

H. A. Abdalla

Department of Mechanical Power Engineering,
Faculty of Engineering, Menoufia University,
Shebin El-Kom, Egypt.

ABSTRACT

This paper presents the effects of surface roughness on the swirling flow characteristics and the swirl decay in conical diffusers. Turbulent swirling flow, with small and moderate swirl intensity, through 8 and 16 degrees included divergence angle diffusers having different wall roughnesses are predicted. The Reynolds-averaged Navier-Stokes equations combined with the k-ε turbulence model, that is valid for both smooth and rough surfaces by incorporating the equivalent sand-grain roughness height into the model functions, are employed in order to calculate the diffuser flows. Three conical diffusers with 8, 12 and 24 degrees divergence angles and having different wall roughness are tested experimentally to clarify the influences of roughness on the diffusers performance. For non-swirling flow, the results indicate that the performance of all diffusers is affeted by increasing the relative wall roughness. Increasing the surface roughness was found to reduce the chances of separation for stalled diffusers. In case of swirling flow, it can be concluded that the rate of swirl decay in conical diffusers is a function of the surface roughness, the total included divergence angle, the diffuser axial length and the inlet Reynolds number. Therefore, the greatest improvement in the performance of rough conical diffuser occurred with an optimum inlet swirl intensity corresponding to the relative surface roughness and the total included divergence angle. The maximum performance of rough conical diffuser is obtained by trading off the effects between relative surface roughness and the swirl intensity. The comparison between predicted and measured results shows that, the numerical model predicts the swirling flow through rough conical diffusers fairly well.

Keywords : Swirling flow, Conical diffusers, Surface roughness, Swirl decay, Performance.

Manuscript received from Dr: H. A. Abdalla at : 8/6/1998,
Accepted at: 30/7/1998,
Engineering research bulletin, Vol. 21, No. 3, 1998, pp. 27-50.
Menoufiya University, Faculty of Engineering,
Shebin El-Kom, Egypt, ISSN. 1110-1180

1- INTRODUCTION

The volute casing of fan, compressor or centrifugal pump is designed precisely so that the static pressure can remain constant over the whole periphery of the impeller. Normally, the surface roughness of the volute may arise from the manufacturing process or from long time of service. Thus the wall surface of the passage is usually not hydraulically smooth and friction between the fluid and the walls of the volute will result in losses. These losses will manifest themselves as a fall in pressure in the direction of flow. This means that a fall in pressure will occur at the origin of the volute, i. e. just after the impeller. In other applications, use of a diffuser downstream of a turbine is useful for energy conservation. For a fixed exit pressure, placing a diffuser at the end of the turbine (gas, steam or hydraulic turbine) reduces the back pressure and increases the turbine pressure ratio and consequently the net output work. The presence of surface roughness will increase the friction losses and affect the flow itself inside the diffuser and consequently it reduces the turbomachine efficiency. Subsequent experiments and correlations have sought relate different types of roughness in different fields to the results of the sand-grain roughness, which are employed in the classical experiments in pipes and boundary layers by Nikuradse [1]. In addition, swirl flow is sometimes observed in the exit pipe of such turbomachines. Therefor, it is necessary to consider the effect of surface roughness in the presence of swirl flow on the performance of conical diffusers. This will be demonstrated in this paper through the study of swirling flow in rough conical diffusers.

Swirling flow in confined geometries is an important subject because of its wide industrial use. Most attention has been given to strongly re-circulating swirling flows in gas turbine combustor geometries or free swirling jets, Refs. [2] to [6]. But swirling turbulent flow in diffusers also occurs in a number of commonly used fluid mechanical devices. For this reasons, many experiments have been performed to analyze which of the effects of swirl on the overall diffuser performance are important for efficient use, Refs. [7] to [9]. In non-swirling diffuser flows, separation or near-separation is caused by the occurrence of a region of low axial momentum near the wall, because of the positive axial pressure gradient. It was found that, the inclusion of swirl upstream of the diffuser inlet can prevent separation occurring for diffuser angles and area ratios at which it would otherwise occur, Refs. [10] and [11]. However, most of these studies concentrate on the effects of swirl intensity and diffuser geometry. Few studies are devoted to the decay of swirling flow in diffusers and no clear generalized methods to predict the decay of swirl along these geometries. One of these few studies was proposed by So [12]. He developed a theoretical model for computing the vortex decay mechanism in a conical diffuser with 6 degrees total included divergence angle. The method based on the solution of integral equations of mass, axial momentum, angular momentum and moment of axial momentum. He concluded that the theoretical results are not compatible with the experimental results. Recently, Abdalla,

et. al. [13] studied the effects of inlet turbulence intensity and inlet swirl on the performance of conical diffusers. They concluded that, the effect of swirling inlet flow on diffuser performance was found to be a strong function of the flow regime in the same diffuser with axial flow. Swirling inlet flow slightly affect the performance of non-separated diffuser flow while swirling inlet flow caused a large improvement for wide-angled diffusers based on inlet swirl intensity. Optima of swirl intensity are presented for the various swirl angles investigated. It is also found that, the decay of swirl is strongly affected by the flow regimes in conical diffusers. On the other hand, effects of Reynolds number on a swirl decay in a circular pipe were measured by many investigators. Kreith and Sonju [14] observed that a turbulent swirl decays to about 10 to 20 percent of its initial intensity in a distance of about 50 pipe diameters. Moreover, the swirl decay being more rapid at smaller than at larger Reynolds number. Hui and Tomita [15] examined experimentally the decay of swirl, the average of dynamic and total pressures and the wall pressure in a long pipeline for two Reynolds numbers and five different inlet swirl intensities. It is found that, the characteristics of swirling flow is a function of swirl intensity, Reynolds number, and pipe length-to-diameter ratio. The effect of surface roughness on the swirl decaying process is neglected in all the previous investigations. The work of Senoo and Nagata [16] is one of the few studies where the swirling flow through pipes with different roughness was considered. They proposed a procedure to compute local wall static pressure and average static pressure if the swirl intensity and the relative roughness of the pipe are specified. Also, an equation for the axial decay of swirl was obtained. Murakami et. al. [17] studied turbulent swirl flows in long straight circular pipes having different wall roughness and discussed the effect of surface roughness on the decay of swirl flow. They found that the strength of the swirl decreases exponentially along the pipe axis and its decrement varies with change of the flow patterns. Murakami et. al. [17] proposed a local relationship between average total pressure and wall pressure. However, these procedures are rather complicated and have limitations. Recently, Reader-Harris [18] was studied the decay of swirling flows in a pipe by solving the simplified Navier-Stokes equations. His results indicated that, the swirl decay rate is increased with increasing the pipe friction factor.

The objective of this work is to study the effects of surface roughness on the characteristics of swirling flow and the swirl decay in conical diffusers. Despite of some previous experimental and numerical studies where surface roughness and pressure gradient are involved, the information that was obtained on this subject still remains far from complete. Also, the process of boundary layer separation with presence of surface roughness is not fully understood. The computational study was made of a conical diffuser with total included divergence angles of 8 and 16 degrees, for the conditions with and without swirl. It is assumed that the flow is steady, axisymmetric and

incompressible. The Reynolds-averaged Navier-Stokes equations combined with the k-ε turbulence model are employed in order to calculate the flow parametes through the diffuser. An experimental evaluation of the effects of surface roughness on the performance of conical diffusers with non-swirling inlet flow was conducted. To verify the numerical method, predicted results are compared with experimental results of conical diffusers with different wall surface roughnesses and different total included divergence angles.

2- THE MATHEMATICAL FORMULATION

2.1 Governing Equations and Turbulence Closure

The problem under consideration is governed by the steady two-dimensional axisymmetric form of the continuity and the time-averaged Navier-Stokes equations. The cylindrical coordinate-system (x, r, θ) is used to describe the flow in the axisymmetric conical diffuser, Fig.(1). For the present study, the steady state equations for incompressible, axisymmetric, turbulent swirling flow may be written as follows, Refs. [19] and [20].

a- Continuity equation : $$\frac{\partial}{\partial x}(\rho u) + \frac{1}{r}\frac{\partial}{\partial r}(\rho v r) = 0 \qquad (1)$$

b- Momentum and turbulence model equations :

The momentum and turbulence model equations in (x, r, θ) directions can be written in the general form as follow,

$$\frac{1}{r}\left[\frac{\partial}{\partial x}(\rho u r \phi) + \frac{\partial}{\partial r}(\rho v r \phi) - \frac{\partial}{\partial x}(r \Gamma_\phi \frac{\partial \phi}{\partial x}) - \frac{\partial}{\partial r}(r \Gamma_\phi \frac{\partial \phi}{\partial r})\right] = S_\phi \qquad (2)$$

The fluxes for the source term S_ϕ are given in table (1), where certain quantities are defined as follows:

$$S^u = \frac{\partial}{\partial x}(\mu \frac{\partial u}{\partial x}) + \frac{1}{r}\frac{\partial}{\partial r}(r \mu \frac{\partial v}{\partial x}) \qquad (3)$$

$$S^v = \frac{\partial}{\partial x}(\mu \frac{\partial u}{\partial r}) + \frac{1}{r}\frac{\partial}{\partial r}(r \mu \frac{\partial v}{\partial r}) \qquad (4)$$

$$G = \mu\left\{2\left[(\frac{\partial u}{\partial x})^2 + (\frac{\partial v}{\partial r})^2 + (\frac{v}{r})^2\right] + \left[\frac{\partial u}{\partial r} + \frac{\partial v}{\partial x}\right]^2 + \left[r\frac{\partial}{\partial r}(\frac{w}{r})\right]^2 + \left[\frac{\partial w}{\partial x}\right]^2\right\} \qquad (5)$$

where, u, v and w are the axial, radial and tangential velocities, respectively. ϕ is the general dependent variable. x, r, and θ are the axial, radial and tangential coordinates. ρ and Γ_ϕ are the density and the effective diffusivity coefficients. S_ϕ is the source of ϕ. In the present calculations, equations were

solved for mean continuity and with dependent variables, ϕ, corresponding to the axial, radial and tangential velocity components. The effective diffusivity was calculated from the two-equations k- ε turbulence model that is valid for both smooth and rough surfaces by incorporating the equivalent sand-grain roughness height into the model functions.

Table 1. The form of the source terms in the general equation (Eq. (1))

ϕ	Γ_ϕ	S_ϕ
1	0	0
u	μ	$-\frac{\partial p}{\partial x}+S^u$
v	μ	$-\frac{\partial p}{\partial r}+\frac{\rho w^2}{r}-\frac{2\mu v}{r^2}+S^v$
w	μ	$-\frac{\rho v w}{r}-\frac{w}{r^2}\frac{\partial}{\partial r}(r\mu)$
k	μ/σ_k	$G-C_D\rho\varepsilon$
ε	μ/σ_ε	$(C_1 G\varepsilon - C_2\rho\varepsilon^2)/k$

The effective viscosity, μ, and the length scale of turbulence motion, ℓ, are given by the following equations, respectively.

$$\mu = \mu_\ell + \rho C_\mu k^2/\varepsilon \qquad (6)$$

$$\ell = C_\mu k^{3/2}/\varepsilon \qquad (7)$$

where μ_ℓ is the laminar viscosity. The standard k-ε turbulence closure model involves five modeling constants, summarized in table (2). These values are recommended by Launder and Spalding [19] based on extensive examination of turbulent flows.

Table 2. Empirical constants in k-ε model

C_μ	C_1	C_2	σ_k	σ_ε
0.09	1.44	1.92	1.0	1.3

2.2 Boundary Conditions and The Effect of Surface Roughness

The governing equations by themselves do not yield a solution to a given problem. Additional boundary information is required at the inlet, outlet, the axis of symmetry and the solid wall. The inlet plane is located for enough upstream the diffuser inlet. Therefore, inlet velocity profiles corresponding to uniform flow were considered at the inlet section. In the case of swirling flows, the swirl velocity profile of a forced vortex was assumed at the inlet section. The turbulence kinetic energy and its rate of dissipation are generally

estimated from the assumption of local equilibrium of turbulence or according to the following expressions, Refs. [21] and [22],

$$k_{in} = a\, u_{in}^2 \quad ; \quad \varepsilon_{in} = k^{1.5} / \lambda d \qquad (8)$$

where d is the diffuser inlet diameter, a and λ are constants. The constants were taken, for the present application, as those given by Lillely and Rhode [21] : a = 0.03 and λ = 0.005. At the outlet plane, the dependent variable or its flux is assumed not to change further in the direction normal to the outlet plane. Either the first or second derivative of a dependent variable in the normal direction is set to zero. The exit plane is located far enough downstream where the flow will not influence the upstream properties. Along the axis of symmetry, the gradient in the radial direction of all variables is set to zero, except for the radial velocity component (v) which is given a definite value of zero.

On the solid boundary, the no-slip velocity boundary conditions are used. In the standard k-ε model, viscous diffusion are neglected and empirical wall functions are used to bridge the viscous layer. This is accomplished by relating the velocity component at the first grid node outside this layer to the wall shear stress via the logarithmic law of the wall. A uniform shear stress prevails in this viscous layer, and the generation and dissipation of energy are in balance there via the assumption that the turbulence is in a state of equilibrium. When local equilibrium conditions prevail in the near-wall layer, the near-wall grid node values of k and ε are fixed to the following empirical correlations via the incorporated logarithmic-law option applicable to smooth walls. The wall functions most commonly used are :

$$k_w = u_\tau^2 / \sqrt{C_\mu} \quad ; \quad \varepsilon_w = u_\tau^3 / (\chi\, y) \quad ; \quad u^+ = \frac{1}{\chi} \ell n(E\, y^+) \qquad (9)$$

where u_τ is the friction velocity, $u_\tau = (\tau_w / \rho)^{0.5}$ and $C_\mu = 0.09$. χ is the Von-Karman constant, taken to be 0.41, and E is the roughness parameter, taken to be 9.7 for smooth wall.

The standard wall functions described above are restricted to smooth walls. Launder and Spalding [19] proposed a wall-function method which can be applied to rough walls as well as smooth walls in which pressure gradient can be accounted. This method is called the generalized wall functions. The main feature of the generalized wall functions is based on a modified log-law that uses the turbulent kinetic energy as the characteristic velocity scale, rather than the friction velocity. The value of k at the near-wall grid cells is not fixed in this option and is calculated from its regular transport equation. However, in the source term for k (Eq. (3)), the dissipation rate for the near-wall cells is fixed to,

$$\varepsilon = C_\mu^{0.75} k^{1.5} \ell n(C_\mu^{0.25} E\, k^{0.5}\, y / \nu) / (2 \chi y) \qquad (10)$$

The principle effects of surface roughness are confined to the inner region of the boundary layer and characterized by the following law of the wall, Ref. [23]

$$u^+ = \frac{1}{\chi}\,\ell n(y^+) + B - \Delta B \quad \text{or} \quad u^+ = \frac{1}{\chi}\,\ell n(E\,y^+) \qquad (11)$$

where $E = \exp(\chi\,(B - \Delta B))$ and ΔB depends on the type and size of roughness, also called the roughness function. For the sand-grain roughness ΔB is found to be a function of k_s^+ ($k_s\,u_\tau / \nu$), where k_s is the absolute roughness height of the sand grain. An empirical formulae given by Jayatillika [24] for E, which express E as a function of the roughness Reynolds number, k_s^+, the value of E could be obtained as follows ;

$$\begin{aligned} k_s^+ &< 3.7 && E = 9.7\text{, the smooth wall value} \\ 3.7 < k_s^+ &< 100 && E = 1/[\,a\,(k_s^+/29.7)^2 + (1-a)/81\,]^{0.5}, \\ k_s^+ &> 100 && E = 29.7/k_s^+ \end{aligned} \qquad (12)$$

where $a = (1 + 2z^3 - 3z^2)$, and $z = 0.02248\,(100 - k_s^+)/(k_s^+)^{0.584}$.

2-3 Numerical Procedure

The governing equations were integrated over the two-dimensional axisymmetric control volume which is created by the cylinderical grid system of coordinates to provide the finite difference equations, Fig. (1). The discretization scheme used is a hybrid system (an upwind-central difference scheme) explained in detail by Launder and Spalding [19]. The set of the resulting algebraic finite-difference equations were solved numerically by an iterative, line-by-line procedure, Ref. [20]. A staggered grid system is employed in the present computation so that the gridlines do not coincide with the diffuser wall. In this method, the diffuser wall surface must be approximated by step-like surfaces, as shown in Fig. (1). For the grid used in calculations, various grid sizes were used to obtain a grid independent solution. The results of calculations show that the grid size 47 x 40 provided grid independent solution. The solution was considered to be converged when the maxima of the mass flux and momentum flux residuals summed at all nodes were less than 0.05 % of the inlet flux.

3- EXPERIMENTAL EQUIPMENT AND PROCEDURE

The arrangement of the experimental test section is shown in Fig. (2). Two electric compressors draw air from the atmosphere to the air tank. The compressor delivery pressure is controlled automatically. The compressed air from the air tank flows through a main pipeline and through a control valve which regulates the flow rate through the test diffusers. In order to cancel out the flow non-uniformity caused by the valve, an entry pipe has 80 diameters length was used before the test diffusers to ensure a fully developed flow at

the entrance. The diffusers have the same entry and exit diameters, 25 mm and 50 mm, respectively. Series of experiments were performed on conical diffusers of total included divergence angles (2α) 8, 12 and 24 degrees. All the tested diffusers are fabricated from copper and having an area ratio (AR) of 4. On leaving the test diffuser, the air enters a tail pipe which passes the air to the atmosphere.

The roughness of the diffuser wall made by sticking three kinds of the sand papers (# 40, # 80 and # 120), which were different in the roughness. The arithmetic center-line average roughness (Ra) of the sand papers was measured at Benha Institute of Technology. The measured values of Ra are given in Table (3). The roughness conditions referred to Ra because the surface roughness of the passage in turbomachines is prescribed by the value of Ra , Ref. [25].

Table 3. Roughness of sand papers used.

Sand papers	# 40	# 80	# 120
Ra (μm)	109.02	53.7	36.1

The experiments were conducted for non-swirling flow through the conical diffusers to verify the numerical study. The diffusers were provided with five static pressure tappings along the surface. The taps of static pressure have 1.0 mm in diameter, were carefully drilled normal to the diffuser surface. In addition to the wall static pressure tap at 3d ahead of the diffuser entrance to measure the reference static pressure. A multi-tube water manometer was used for measuring the pressure recovery coefficient along the tested diffusers. The measurements of inlet velocity profiles at 3d ahead of the diffuser entrance were conducted using a calibrated three holes probe. The pressure recovery coefficient, C_P, which is a measure of the diffuser efficiency is expressed in terms of the actual static pressure rise (ΔP) to the inlet dynamic pressure ($0.5 \rho U_{in}^2$), $C_P = \Delta P / (0.5 \rho U_{in}^2)$. The air velocity at the entrance of the tested diffuser was measured using a calibrated three holes probe. Experiments were carried out for the inlet Reynolds number (Re) ranged from 5×10^4 to 1.72×10^5 , based on the inlet mean velocity and the inlet diameter of the diffuser.

The uncertainties of the measurements of the inlet velocity profiles are estimated to be about ± 1.5 percent. The experimental errors in the pressure measurements and the pressure recovery coefficient are estimated to be about ± 0.5 and ± 1.2 percent, respectively. The experimental errors in the measurements were calculated using Kline and McClintock technique [26].

4- COMPUTATIONAL RESULTS

4-1 Results of Non-Swirling Flow in Rough Diffusers

Figure (3) indicates the axial variation of the wall pressure recovery coefficient (C_p) with x/L_d for two conical diffusers with total included divergence angle 2α = 8 and 16 degrees and having an area ratio of 4, respectively. The effect of relative surface roughness ($\bar{k}_s$) on the variation of pressure recovery coefficient at constant Reynolds number of 1.1×10^5 has been plotted in the figures. For smooth and rough diffusers, the results indicate that there is an increase in the pressure recovery coefficient with an increase in x/L_d . However, the rate of increase of C_p with x/L_d decreases near to the diffuser exit. The curves for various values of relative roughness are almost identical to the curve for zero-relative roughness or smooth surface condition. It can be observed from these figures that, the pressure recovery coefficient for both diffusers seems to be very sensitive to the surface roughness variation from the beginning of the diffuser. Generally, the pressure recovery coefficient of 8 and 16 degrees diffusers are decreased with increasing the relative roughness of the diffuser wall. The resultant effect of increasing $\bar{k}_s$ is a large drop in the C_p at the entrance of the diffuser and a more significant reduction in the C_p at the diffuser exit. This occurs due to an increase in the boundary layer blockage at the diffuser inlet which reduces the effective flow area, in addition to increasing the friction losses with increasing the surface roughness. It was pointed out that in smooth ducts friction losses were completely determined by the Reynolds number. In rough ducts, the value of friction factor depends also on the roughness of the inside surface.

In 16 degrees diffuser, as shown in Fig. (4), it is noticed at constant surface roughness that, the velocity near to the diffuser wall decreases as the flow moves downstream and hence the wall pressure increases. The kinetic energy of the particles of the fluid enables them to move against the growing pressure and the friction resistance. The degradation of kinetic energy is along the diffuser and from the centerline to the boundary. The energy of layers at the boundary is so small that the increased pressure may stop the flow there or even reverse it. As a result, eddies form and the flow separation from the wall, as shown in Fig. (4) which displays the variation of the normalized wall velocity with x/L_d for smooth and rough conditions. It is noticed from this figure that, the smooth wall velocity distribution shows faster rate of decay than the rough wall velocity distribution along the diffuser. Increasing the relative roughness of the surface up to 0.009259 is accompanied by an increase in the wall velocity and hence the separation is suppressed. This is referred to that, increasing the surface roughness will increases also the turbulence level in the wall region, as shown in Fig. (5), and hence the turbulence loss will be decreased. The high turbulence level in the wall region results in a decrease of the distortion within the diffuser, as shown in Fig. (6) which is plotted at $x/L_d = 0.966$. This will control the boundary layer growth

along the diffuser wall and consequently reduces the separation tendency. In spite of the disappearance of the separation tendency with increasing the surface roughness, the overall pressure recovery coefficient of 16 degrees diffuser is noticed to decrease. This may be attributed to the reduction of the effective flow area that caused by the increase of the boundary layer blockage at the diffuser entrance and the surface roughness. Three other references also clearly demonstrate a reduction of C_P owing to an increase in the inlet blockage of the boundary layer, in spite of high turbulence; Ref. [27], when a screen ring enlarged the wake component of the velocity profile, Ref. [28]; when a rough entrance pipe was employed and Ref. [29], when the entrance plane contained annular steps. On examining the non-dimensional axial velocity distribution near the diffuser exit, as plotted in Fig. (6), one observes that the separation tendency is completely disappeared when the relative surface roughness of the diffuser wall becomes 0.009259.

4-2 Results of Swirling Flow in Rough Diffusers

The effect of relative surface roughness on the wall pressure recovery coefficient along 8 degrees diffuser is plotted in Fig. (7) for two swirling flow intensities at the diffuser inlet, S_o = 0.0906 and 0.2965. Local swirl number (S) has been successfully used to express the swirl intensity by several investigators, Senoo et. al. [11] and Algiferi et. al. [30]. It is defined as the ratio of the angular momentum flux to the product of the inlet radius and the axial momentum flux. The swirl number (S) may be defined as :

$$S = \int_0^R u\, w\, r^2\, dr \;/\; R_{in} \int_0^R u^2\, r\, dr \qquad (13)$$

where u and w are axial and tangential velocities, respectively, R_{in} is the inlet diffuser radius. In the present calculations, four swirl intensities 0.0, 0.0906, 0.1869 and 0.2965, which are equivalent to swirl angle β = 0, 10, 20 and 30 degrees, were tested. It can be observed from Fig. (7) that, by increasing the relative surface roughness, the pressure recovery coefficient was found to be dramatically reduced in spite of the presence of swirling flow. The same trend is also observed for 16 degrees diffuser, as shown in Fig. (8). The main reason of lowering the pressure distribution along the diffusers is the increase of frictional losses because of the greater surface area in the case of swirling flow. In addition, increasing the surface roughness may be absorbing the swirl effect and it increases the rate of swirl decay. In the case of 16 degrees diffuser, it can be seen from Fig. (9-a) that a low velocity region with reversal flow occurs at the diffuser exit when the inlet swirl intensity is 0.0906 and $\bar{k}_s$ = 0.0 . With the introduction of lightly swirling flow (S_o = 0.0906), the tendency of flow separation increases with increasing the relative surface roughness. Large inlet swirl intensity was necessary in order to reduce or to eliminate the separation zone and then improving the pressure recovery. This was observed in Fig. (9-b) where the separation is eliminated completely from

the 16 degrees diffuser with the smooth surface condition as the swirl intensity increased to 0.2965. This may be attributed to the resulting radial pressure gradient which bring about enhanced the fluid mixing near the boundary and decreases the boundary layer thickness. As a consequence, the pressure recovery at the diffuser exit is increased, compare Figs. (8-a) and (8-b). However, increasing the surface roughness from 0.0 to 0.005556 increases again the separation tendency inside the diffuser as shown in Fig. (9-b). This means that the magnitude of optimum swirl intensity, i.e. the swirl at which the pressure recovery is the maximum, is strongly depends on the relative surface roughness in addition to the total included divergence angle of the diffuser. The results of C_p variations plotted in Figs. (10) and (11) indicate that the optima of inlet swirl intensity required for obtaining the maximum improvement in the pressure recovery was not the same for the tested diffusers at different surface roughness. As shown in Fig. (11), the optimum swirl intensity for the maximum pressure recovery coefficient of 16 degrees diffuser is approximately 0.2965 and 0.378 for the relative surface roughness of 0.000756 and 0.005556, respectively. It was found also that the separation in the diffuser with rough surface ($\overline{k}_s = 0.005556$) is completely suppressed when a swirl with an optimum intensity of 0.378 is imparted to the flow at the diffuser inlet, as shown in Fig. (12). However, subjecting a diffuser to a swirl larger than optimum swirl would lead to a deterioration in its performance due to the formation of re-circulation zone along the diffuser centerline, Refs. [11] to [13]. By comparing Figs. (6) and (12), it is clearly observed that the presence of swirling flow reduces the value of relative surface roughness required for eliminating the flow separation in 16 degrees diffuser. It can be seen also from the comparison that, the fluid pressed towards the wall and suppresses the formation of separation in swirling flow cases. However, as shown in Fig. (12), for a certain value of $\overline{k}_s$ ($\overline{k}_s = 0.005556$) increasing the swirl intensity reduces the centerline velocity which increasing the pressure recovery of the diffuser. When the swirl intensity is greatly elevated, a re-circulation zone may be created along the centerline near the diffuser exit. As a consequence, the pressure recovery coefficient will be decreased due to the reduction of the effective cross sectional area. On the other hand, in non-swirling flow, the centerline velocity increases as the surfaces roughness increases, as shown in Fig. (6), and consequently results in a low pressure recovery coefficient. In general, the results suggested that the separation flow can be prevented either by adding a swirl with suitable intensity to the axial flow or by roughening the diffuser wall. However, prevention of separation due to swirl caused the performance to increase. Finally, it can be concluded that, the maximum performance of rough conical diffuser is obtained by trading off the effects between relative surface roughness and the swirl intensity.

In order to examine the influence of the relative surface roughness on the swirl decay, the variation of the relative local swirl intensity $\overline{S}$ (S/S_o) along

the diffuser centerline is shown in Fig. (13) for 8 degrees diffuser and in Fig. (14) for 16 degrees diffuser. The results of the swirl decay are plotted for two different inlet swirl intensities, namely S_o = 0.0906 and 0.2965, while the relative surface roughness is varied from 0.0 to 0.005556. Generally, the relative swirl intensity $\bar{S}$ at upstream stations is large and it decreases continuously along the diffuser centerline. It is clear from these figures that the swirl decay depends on the relative surface roughness and the total included divergence angle of the diffuser. The main observation which can be observed from these figures is that, the rate of swirl decay in the 8 degrees conical diffuser is more than that in the case of 16 degrees conical diffuser. For smooth surface conditions, it is noticed that a turbulent swirl decays to about 20 percent of its initial swirl intensity in 8 degrees diffuser and to about 15 percent in 16 degrees diffuser, for the same inlet conditions. The swirl decay through the 8 degrees diffuser increases from 20 percent to about 55 percent of its initial intensity as the relative surface roughness increases from 0.0 to 0.005556, while the swirl decay increases from 15 percent to about 35 percent of its initial intensity in the case of 16 degrees diffuser. This means that the surface roughness absorbs the swirl effects and accelerates the swirl decay because the wall friction reduces the angular momentum of swirl flow.

The effect of inlet Reynolds number on the swirl decay in the same diffusers is examined for the smooth and rough diffusers at S_o = 0.2965. Two Reynolds numbers of 0.5×10^5 and 1.1×10^5 were used in the present computations. In the case of smooth diffusers, the axial swirl decay for 8 and 16 degrees diffusers is presented in Figs. (15-a) and (15-b), respectively. An inspection of these figures shows that the rate of decay depends on the inlet Reynolds number. The decay rate increases as the Reynolds number decreases. The same conclusion has been achieved by Kreith and Sonju [14] for the case of swirling flow in pipes. For smooth surface conditions, the rate of swirl decay in 8 degrees diffuser is greater than that of 16 degrees diffuser for both Reynolds numbers. This may be due to the presence of flow separation in addition to the shorter length of 16 degrees diffuser compared to that of 8 degrees diffuser. For rough diffusers and at constant surfae roughness ($\bar{k}_s$ = 0.002385), it can be observed from Figs. (16) that the rate of swirl decay is reduced with decreasing the inlet Reynolds number. Generally, it was found that, the swirl decay across the 16 degrees diffuser is slightly affected by the inlet Reynolds number in both smooth and rough cases, but it strongly depends on the diffuser length. This is due to the strong adverse pressure gradient which creates in wide-angled diffusers.

To summarize, the overall performance of conical diffusers which is measured by the overall pressure recovery coefficient at the diffuser exit (C_{Po}) is presented in Figs. (17-a) and (17-b) for 8 and 16 degrees total included divergence angles, respectively. In these figures, the results are plotted to indicate the effect of surface roughness on the overall pressure

recovery coefficient at different swirl intensities, S_o = 0.0, 0.0906, 0.186 and 0.2965. The inlet Reynolds number for both diffusers was held constant at 1.1×10^5 . The results indicate that the overall pressure recovery coefficient seems to be very sensitive to the relative surface roughness and the inlet swirl intensity. As discussed previously, it is observed for both diffusers that, the overall pressure recovery coefficient decreases as the relative surface roughness increases. The same trends are shown for both non-swirling and swirling flow. An examination of these figures indicate that the greatest improvement in the performance of each diffuser occurred with an optimum swirl intensity corresponding to the flow regime and the relative surface roughness. This is referred to that, the swirl decaying is increased with increasing the relative surface roughness.

5- COMPARISON OF THEORETICAL AND EXPERIMENTAL RESULTS

To verify the numerical method, predicted results are compared with experimental results of conical diffusers with different surface roughness and different total included divergence angles for non-swirling flow conditions. These measurements are conducted at the heat engine laboratory, Faculty of Engineering, Shebin El-Kom. In order to examine the influence of the wall roughness on the performance of conical diffusers, three diffusers with different roughnesses were used. In the case of non-swirling inlet flow, Fig. (18) shows a comparison between the calculated values of the axial pressure recovery coefficient and the measurements for three conical diffusers with total divergence angle of 8, 12 and 24 degrees. The comparison is conducted at a Reynolds number of 1.72×10^5 . The values of the inlet blockages of the boundary layer were found in the range 0.1 to 0.35. This means that the inlet boundary layer thickness is changed from thin to thick inlet boundary layer according to the surface roughness. Therefore, it can be concluded that the upstream pipe roughness as well as Reynolds number are important parameters in determining the probable performance of a conical diffuser, and that in many practical cases diffusers will operate with much thicker inlet boundary layers. The results indicate that the theory predicts the pressure recovery coefficient fairly well. The early departure of the theoretical curves from experimental points at the diffuser entry can be attributed to the effects of the sharp junction between the inlet pipe and tested diffusers. However, the figures indicate a good qualitative agreement between the theory and experimental results for all diffusers.

For swirling flow, the predicted values are compared with measurements made by Neve and Wirasinghe [10] for five conical diffusers with different total included divergence angles and an outlet to inlet area ratio of 4.0. The inlet Reynolds number was 0.466×10^5 . Inlet conditions of axial velocity and swirl velocity were taken from measured values. Unfortantually, no available existing experimental data for rough conical diffusers with inlet swirling condition can be used for comparison purpose. For swirling flow and smooth

surface condition, the experimental data of Neve and Wirasinghe [10] are used for comparison purposes. The measurements were conducted with five different conical diffusers of total divergence angles of 10, 15, 20, 25 and 30 degrees to clarify the influence of swirl on the performance of conical diffusers. Four swirl intensities equivalent to swirl angle $\beta = 0.0, 8.6, 10.9$ and 15 degrees were tested for each diffuser configuration. The effect of inlet swirl intensity on the C_{Po} for all tested diffusers in the Ref. [10] is shown in Fig. (19). The flow with additional amounts of swirl is numerically simulated and the predicted results are compared with the experimental data for all tested diffusers. The results indicate that the addition of a swirl to an axial flow in a conical diffuser can lead to improvements in C_{Po}. The predictions are in good agreement with the experimental results.

6- CONCLUCTIONS

The swirling flow in rough conical diffusers is investigated theoretically and experimentally to clarify the influences of roughness on the diffuser performance and the swirl decay. The main results obtained are :

1- The axial pressure recovery (C_p) of all tested conical diffusers is decreased with increasing the relative surface roughness ($\bar{k}_s$) for non-swirling inlet flow. The resultant effect of increasing $\bar{k}_s$ is a large drop in the C_p at the entrance of the diffuser and a more significant reduction in the C_p at the diffuser exit.

2- Increasing the surface roughness was found to have an effect on the separation phenomenon for moderate stalled diffusers, due to the increase of turbulence intensity in the wall region.

3- The optimum inlet swirl intensity for the maximum improvement in the overall pressure recovery coefficient is strongly depends upon the surface roughness and the total included divergence angle of the diffuser. The good performance of rough conical diffuser is obtained by treading off the effects between relative surface roughness and the swirl intensity.

4- The rate of swirl decay in conical diffusers is a function of the surface roughness, the total included divergence angle, the diffuser axial length and the inlet Reynolds number. It was found that, the surface roughness accelerates the swirl decay, while the rate of swirl decay in small angle diffuser is more than that in the large angle diffuser. On the other hand, the swirl decay in small angle diffuser increases as the inlet Reynolds number decreases, but the swirl decay across the large angle diffuser is slightly affected by the inlet Reynolds number in both smooth and rough cases.

5- The numerical model is suited to predict the swirling flow through smooth and rough diffusers.

NOMENCLATURE

AR	diffuser area ratio
C_p	local pressure recovery coefficient
C_{Po}	overall pressure recovery coefficient across the diffuser, $C_{Po} = \Delta P_o / 0.5\ \rho\ U_{in}^2$
d	diffuser inlet diameter
k_s	absolute surface roughness
$\bar{k}_s$	relative absolute roughness, $\bar{k}_s = k_s / d$
k_w	turbulence kinetic energy near the wall
L_d	the axial diffuser length
L_e	the entry pipe length
L_t	the tail pipe length
R	local diffuser radius
Re	inlet Reynolds number, $Re = U_{in}\ d / \nu$
S	local swirl intensity
S_o	inlet swirl intensity
$\bar{S}$	the relative local swirl intensity, $\bar{S} = S / S_o$
U_{in}	inlet velocity
u, v, w	axial, radial and tangential velocities
u_w	the axial velocity near the wall
x, r, θ	axial, radial and tangential coordinates
y	normal coordinate measured from the diffuser wall
ΔP_o	static pressure difference between diffuser exit and entrance
α	half-total included divergence angle
β	inlet swirl angle
ν	kinematic viscosity

REFERENCES

1- Nikuradse, J., "Laws of Flow in Rough Pipes", NACA TM 1292, 1950.

2- Lillely, D. G., "Combustor Swirl Flow Modelling", AIAA J., No. 8, April 1975, pp. 419.

3- Lillely, D. G., "Primitive Pressure-Velocity Code for The Computation of Strongly Swirling Flow", AIAA J., Vol. 14, No. 6, June 1976, pp. 749.

4- Okhio, C. B., Horton, H. P. and Langer, G., "Calculation of Turbulent Swirling Flow Through Wide Angle Conical Diffusers and The Associated Dissipative Losses", Int. J. Heat Fluid Flow, Vol. 7, No. 1, Mar. 1986, pp. 37.

5- Yung-Chain-Nan, "Numerical Simulation of Axisymmetric Turbulent Flow in Combustors and Diffusers", NASA Report 4115, Feb. 1988.

6- Sen Nieh and Jian Zhang, "Simulation of The Strongly Swirling Aerodynamic Flied in a Vortex Combustor", Trans. ASME, J. of Fluids Engg., Vol. 114, Sept. 1992, pp. 367.

7- McDonald, A. T., Fox, R. W., and Van Dewoestine, R. V., "Effects of Swirling Inlet Flow on Pressure Recovery in Conical Diffusers", AIAA J., Vol. 9, Oct. 1971, pp. 2014.
8- Steven W. Armfiled, Nam-Hyo Cho and Clive A. J. Fletcher, "Prediction of Turbulence Quantities for Swirling Flow in Conical Diffusers", AIAA J., Vol. 28, No. 3, March 1990, pp. 453.
9 - Clausen, P. D., Koh, S. G., and Wood, D. H., "Measurements of a Swirling Turbulent Boundary Layer Developing in a Conical Diffuser", Experimental Thermal and Fluid Science J., Vol. 6, No. 2, 1993, pp. 39.
10- Neve, R. S. and Wirasinghe, N. E. A., "Changes in Conical Diffuser Performance by Swirl Addition", Aero. Quarterly J., Vol. 8, Aug. 1978, pp. 131.
11- Senoo, Y., Kawaguchi, N., and Negata, T., "Swirl Flow in Conical Diffusers", Bulletin of the JSME J., Vol. 21, No. 151, 1978, pp. 112.
12- So, K. L., "Vortex Phenomena in a Conical Diffuser", AIAA J., Vol. 5, June 1967, pp. 1072.
13- Abdalla, H. A., El-Mayit, M. M., Khalifa, B. A. and El-Shazly, A. M., "Effects of Inlet Turbulence Intensity and Inlet Swirl on Diffuser Flows", Engg. Research Bulletin, Menoufia University, Faculty of Engg., Shebin El-Kom, Egypt, Vol. 19, No. 2, May-June 1996, pp. 49.
14- Kreith, F. and Sonju, O. K., "The Decay of a Turbulent swirl in a Pipe", J. Fluid Mechanics, Vol. 22, 1965, pp. 257.
15- Hui Li and YuJi Tomita, "Characteristics of Swirling Flow in a Circular Pipe", ASME, J. Fluid Engg., Vol. 116, June 1994, pp. 370.
16- Senoo, Y. and Nagata, T., "Swirl Flow in Long Pipes With Different Roughness", Bulletin of the JSME J., Vol. 15, No. 90, 1972, pp. 1514.
17- Murakami, M., Kito, O., Katayama, Y. and Iida, Y., "An Experimental Study of Swirling Flow in Pipes", Bulletin of the JSME J., Vol. 19, No. 128, Feb. 1976, pp. 118.
18- Reader-Harris, M. J., "The Decay of Swirl in a Pipe", Int. J. Heat and Fluid Flow, Vol. 15, No. 3, June 1994, pp. 212.
19- Launder, B. E. and Spalding, D. B., "The Numerical computation of Turbulent flows", Computer Methods in Applied Mechanics and Engineering, Vol. 3, 1974, pp. 269.
20- Gosman, A. D. and Pun, W. M., "Calculation of Re-circulating Flows", Rept. No. HTS/74/12, Dept. of Mech. Engg., Imperial College, London, England, 1974.
21- Lillely, D. G. and Rhode, D. L., "A Computer Code for swirling Turbulent Combustor Geometries", NASA Contractor, Report 3442, 1982.
22- Pourahamdi, F. and Humphrey, J. A. C., "Prediction of Curved Channel Flow With an Extended k-ε Model of Turbulence", AIAA J., Vol. 21, 1983, pp. 1365.
23- Patel, V. C. and Yoon, J. Y., "Application of Turbulence Models to Separated Flow Over Rough Surfaces", Trans. ASME, J. of Fluids Engineering, Vol. 117, June 1995, pp. 234.

24- Jayatillika, C. I. V., "The Influence of Prandtle Number and Surface Roughness on The Resistance of The Laminar Sublayer to Momentum and Heat Transfer", Prog. in Heat and Mass Transfer, Vol. 1, Pergamon Press, 1969.
25- Taylor, R. P., "Surface Roughness Measurements on Gas Turbine Blades", Trans. ASME, J. of Turbomachinery, Vol. 117, 1990, pp. 175.
26- Kline, S. J. and McClintock, F. A., "Describing the Uncertainties in Single-Sample Experiments", ASME, Mechanical Enginreeing Journal, Vol. 1, 1953, pp. 3.
27- Sajben, M., kroutil, J. C., and Sedrick, A. V., "Conical Diffuser Flows With Natural and Screen-Simulated Inlet Conditions", AIAA J., Vol. 14, No. 12, Dec. 1976, pp. 1723.
28- Bradely, I. C., and Cockrell, D. J., "The Response of Diffusers to Flow Conditions at Their Inlet", Symposium on Internal Flows, University of Salford, England, 1971, paper 5.
29- Miller, D., "Performance of Straight Diffusers", Part II of "Internal Flow : A Guide to Losses in Pipe and Duct Systems", B. H. R. A. Fluid Engg., Cranfield / Bedford, 1971.
30- Algiferi, A. H., Bhardwaj, R. K., and Rao, Y. V. N., "Prediction of The Decay Process in Turbulent Swirl flow", Proceeding of Institution of Mechanical Engineering, Vol. 201, 1987, pp. 279.

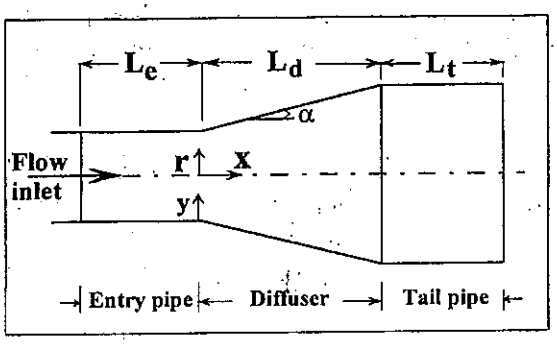

a)

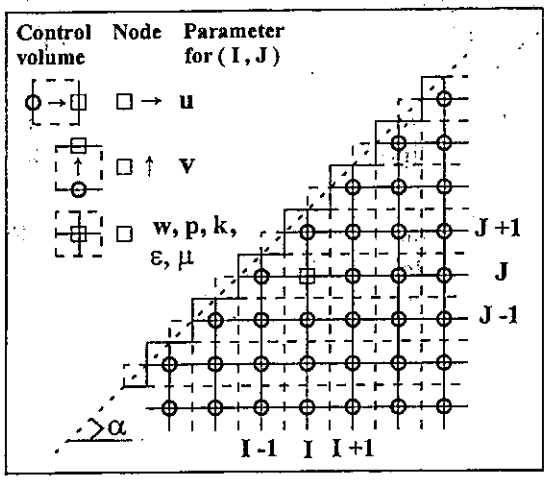

b)

Figure 1 Staggered grid distribution and control volume for conical diffuser

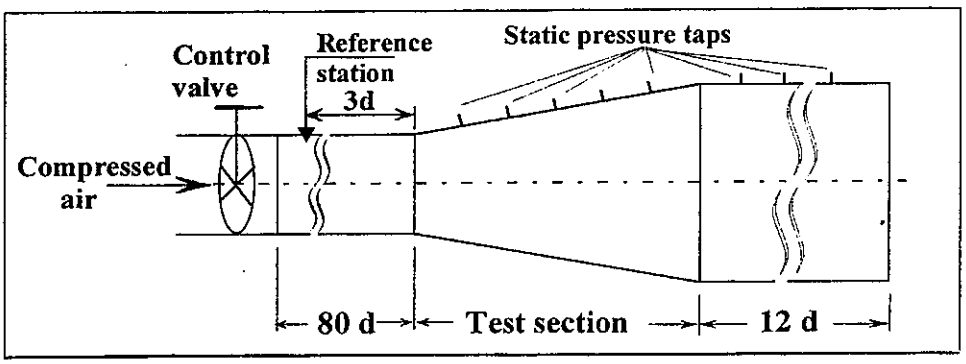

Figure 2 Layout of the test section

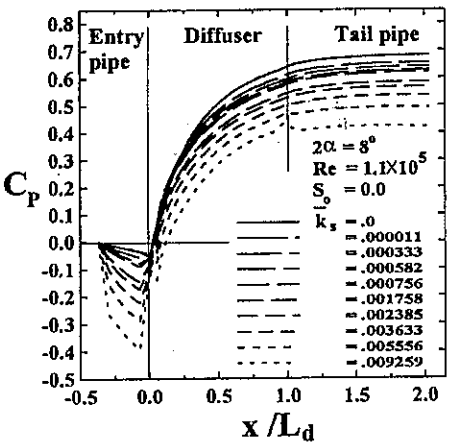

a)

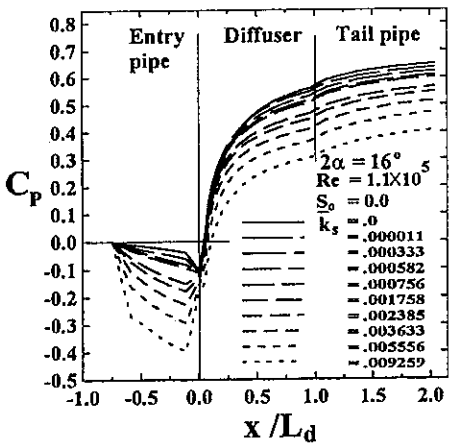

b)

Figure 3 Axial variation of C_p with $\bar{k}_s$ for a non-swirling flow

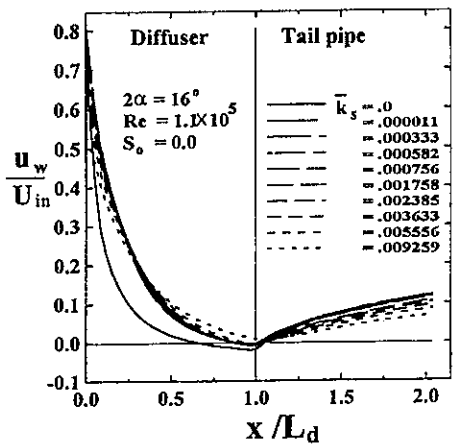

Figure 4 Axial variation of near wall velocity with $\bar{k}_s$ for 16 deg. diffuser

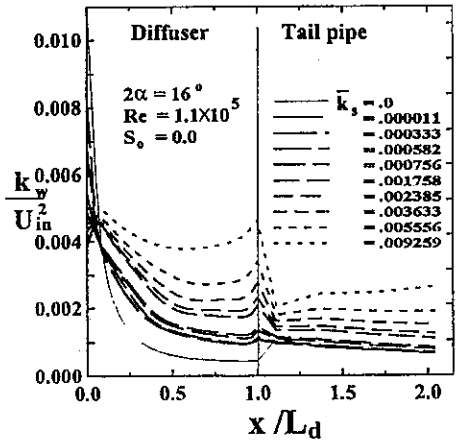

Figure 5 Axial variation of turbulence intensity with $\bar{k}_s$ for 16 deg. diffuser

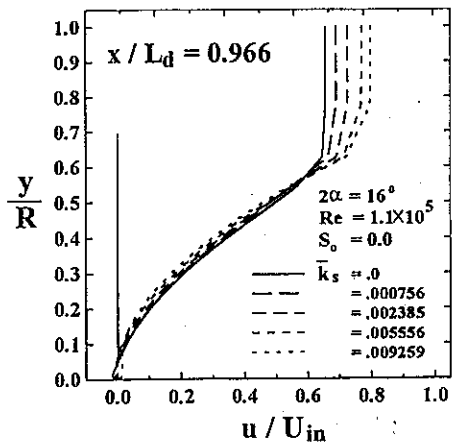

Figure 6 Radial distribution of axial velocity with $\bar{k}_s$ for 16 deg. diffuser

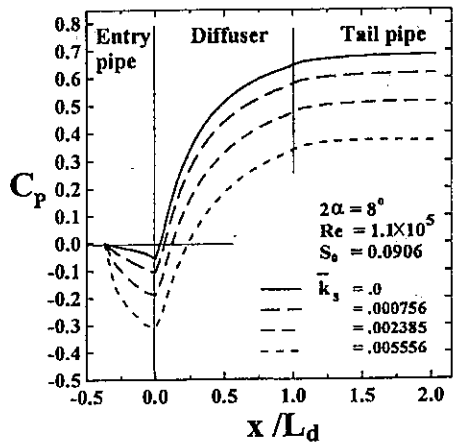

Figure 7- a

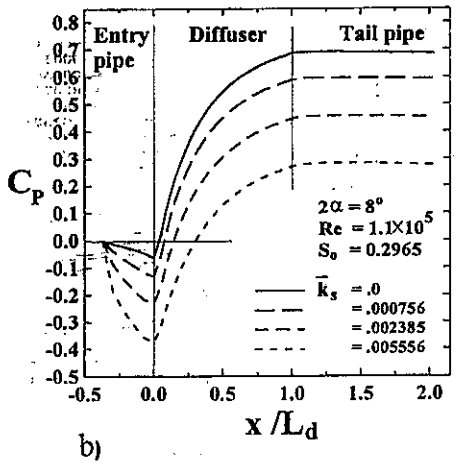

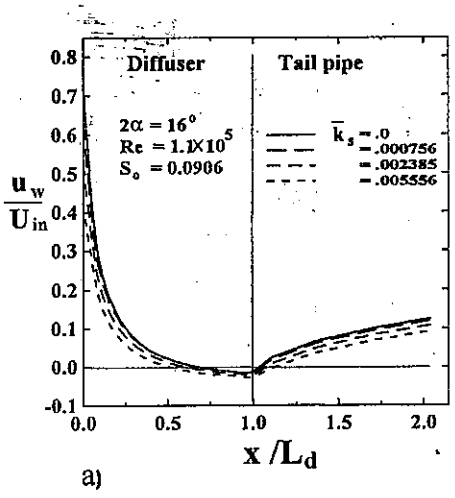

Figure 7 Axial variation of C_p with $\bar{k}_s$ for different S_o

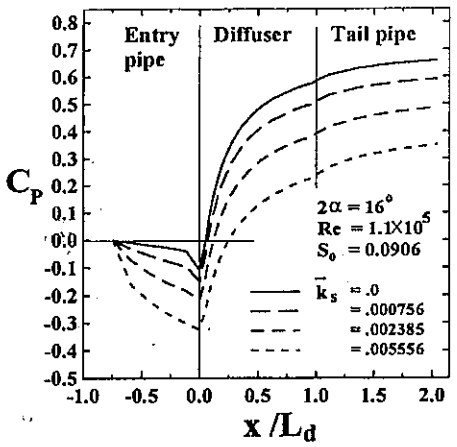

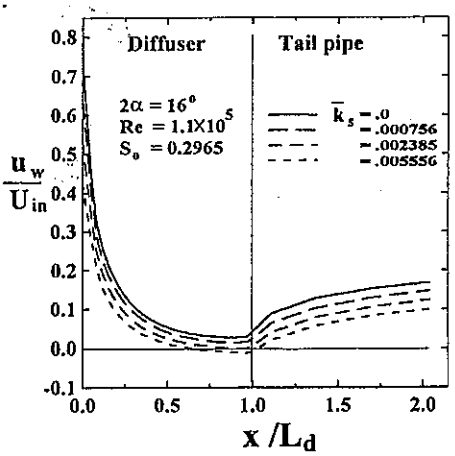

Figure 9 Axial variation of near wall velocity with $\bar{k}_s$ different S_o

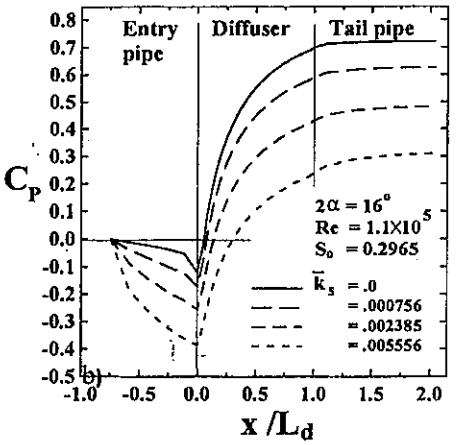

Figure 8 Axial variation of C_p with $\bar{k}_s$ for swirling flow in 16 deg. diffuser

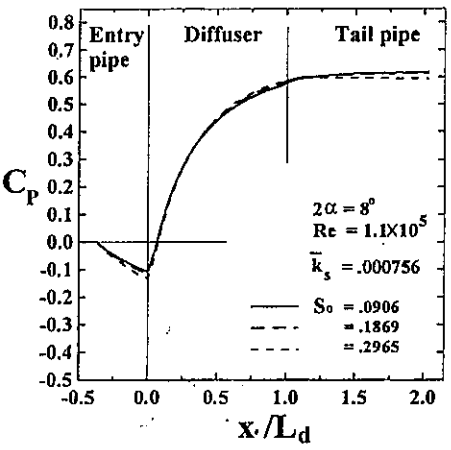

Figure 10- a

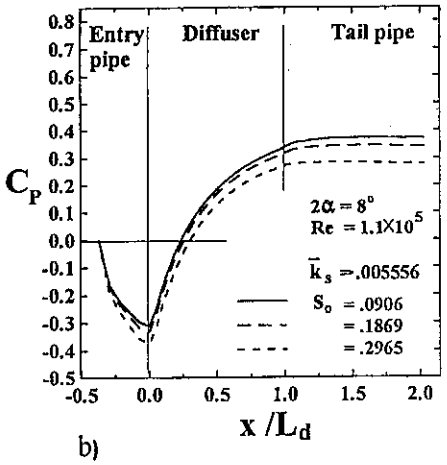

Figure 10 Effect of S_o on C_P variation for different $\bar{k}_s$, (8 deg. diffuser)

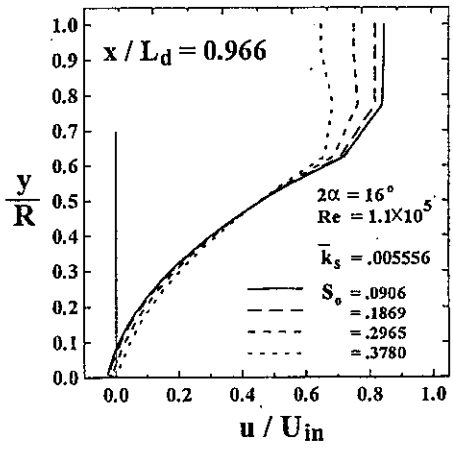

Figure 12 Radial variation of axial velocity in 16 deg. diffuser at different swirl intensities

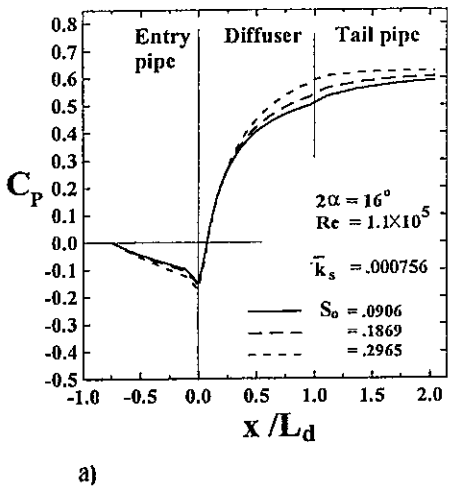

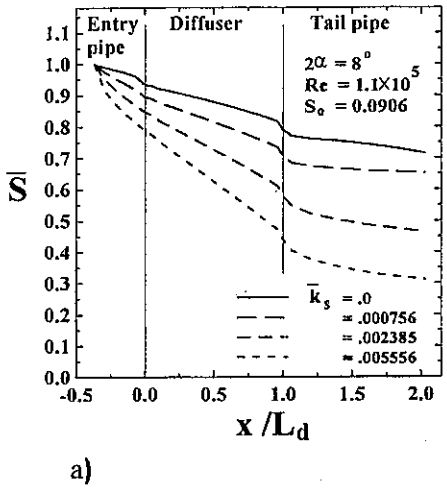

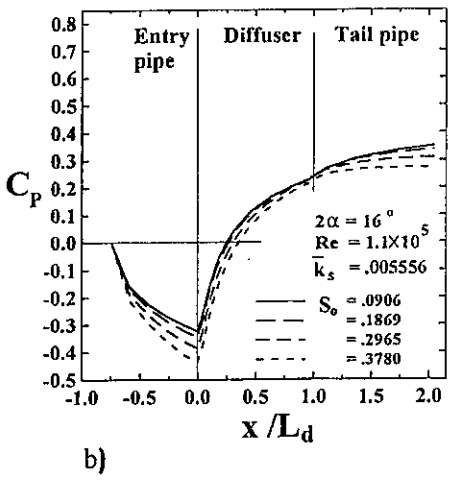

Figure 11 Effect of S_o on C_P variation for different $\bar{k}_s$, (16 deg. diffuser)

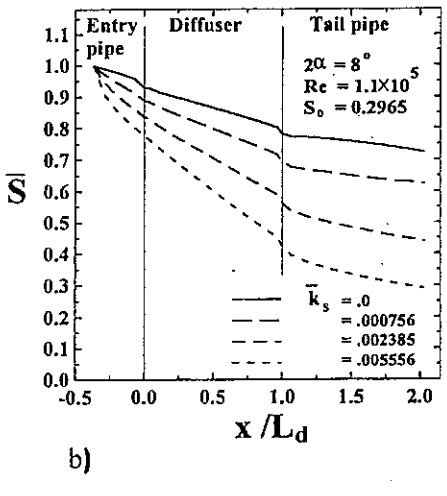

Figure 13 Axial swirl decay in 8 deg. diffuser for various $\bar{k}_s$ and S_o

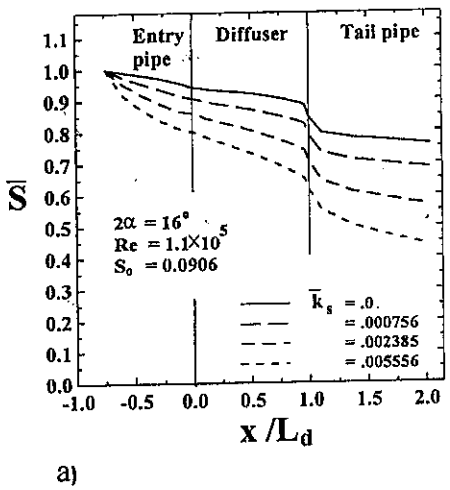

a)

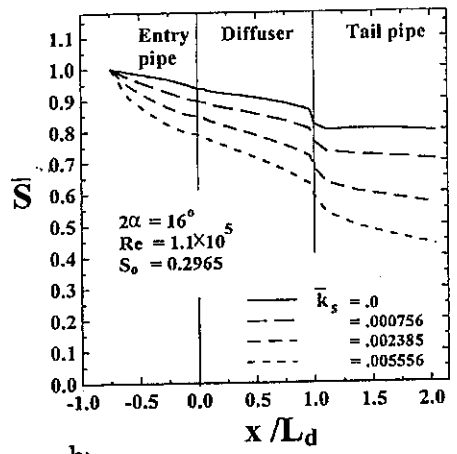

b)

Figure 14 Axial swirl decay in 16 deg. diffuser for various $\bar{k}_s$ and S_o

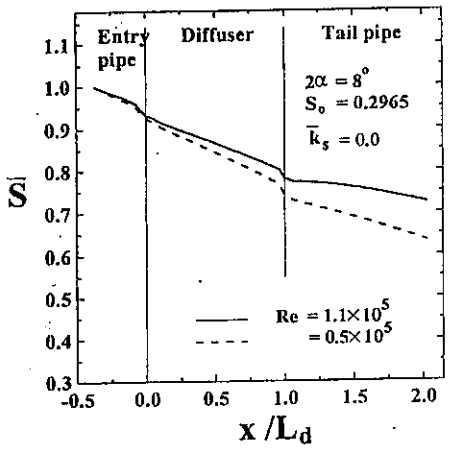

Figure 15 – a

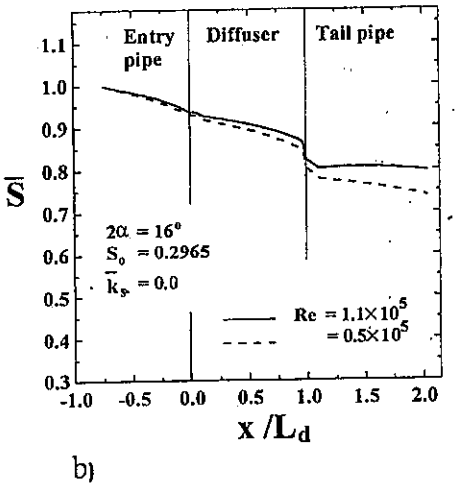

b)

Figure 15 Effect of Re on the axial swirl decay in smooth diffusers

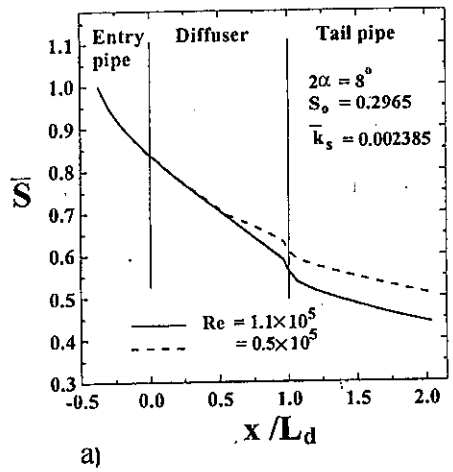

a)

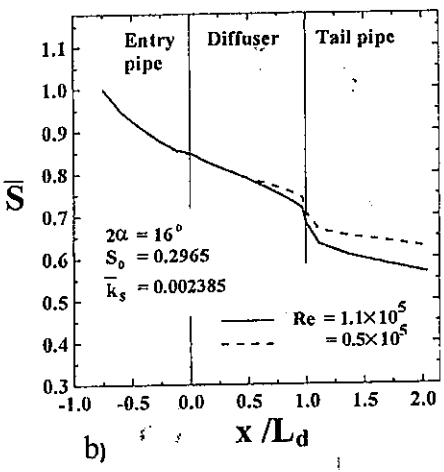

b)

Figure 16 Effect of Re on the axial swirl decay in rough diffusers

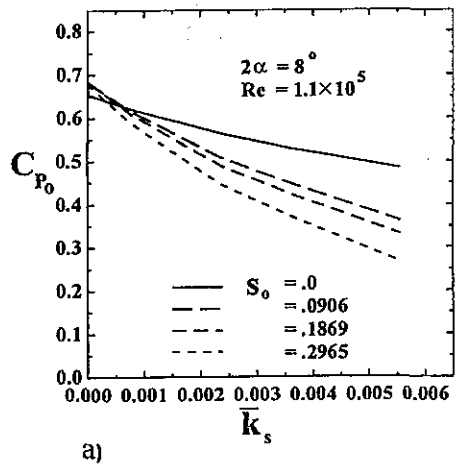

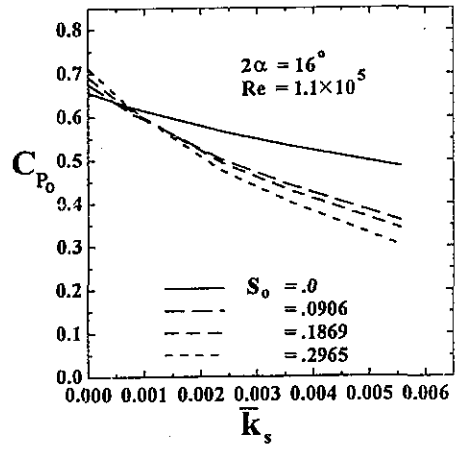

Figure 17 Variation of C_{Po} with $\bar{k}_s$ at various swirl intensities

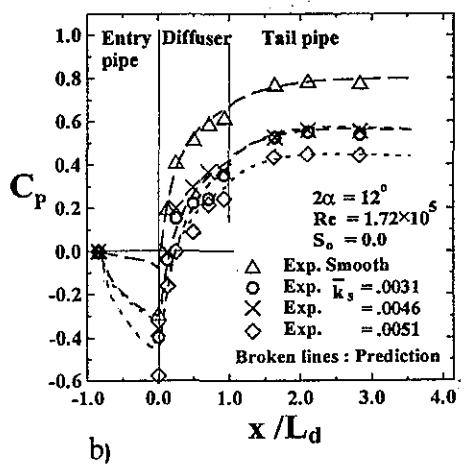

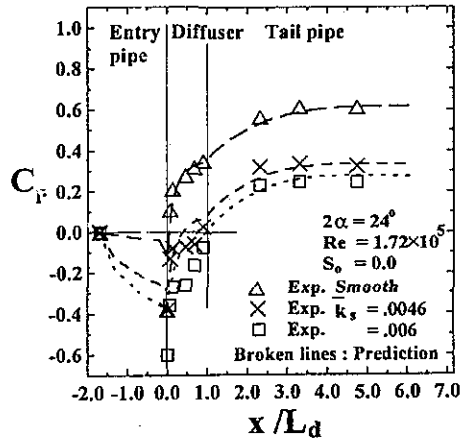

Figure 18 Comparison between predicted and measured C_P for smooth and rough diffusers

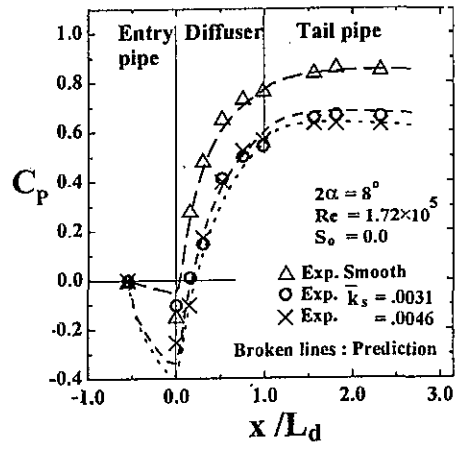

Figure 18 - a

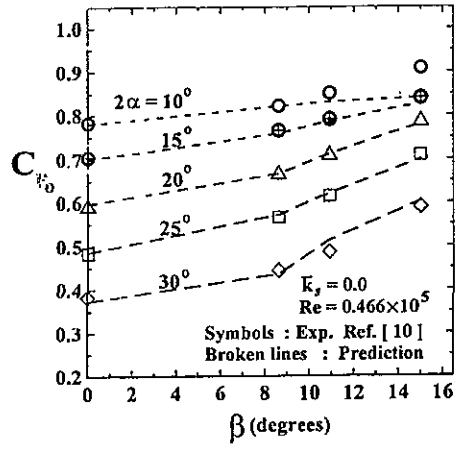

Figure 19 Comparison between predicted and measured C_{Po}, Ref. [10]

عنوان البحث : السريان الدوامى فى النواشر المخروطية المخشنه

د. / حسن عوض عبد الله

قسم هندسة القوى الميكانيكية –كلية الهندسة – شبين الكوم

ملخص البحث :

هذا البحث يتناول دراسة نظرية ومعملية لتأثير خشونة السطح على خصائص السريان الدوامى وإضمحلاله فى النواشر المخروطية. تمت الدراسة النظرية على نواشر مخروطية ذات زاوية إنفراج ٨، ١٦ درجة، وكذلك أجريت الدراسة المعملية على نواشر ذات زاوية إنفراج ٨، ١٢، ٢٤ درجة.

أجريت الدراسة النظرية لسريان إضطرابى دوامى عند شدة دوامية مختلفة وكذلك لدرجة خشونة متعددة. كذلك تم دراسة تأثير رقم الرينولدز على إضمحلال السريان الدوامى فى النواشر ذات السطوح الخشنة. بنيت الدراسة النظرية على حل النموذج الرياضى للمعادلات الحاكمة للسريان (معادلات كمية التحرك، الإستمرارية، نموذج الإضطراب للسريان مأخوذ فى الإعتبار تأثيرخشونة السطح). ولتحقيق النموذج الرياضى تم إجراء التجارب المعملية على نواشر مخشنة وغير مخشنة. تم تخليق خشونة السطح بلصق ورق من النوع المحبب بالرمل على السطح الداخلى للنواشر.

أظهرت النتائج النظرية للسريان الغير دوامى فى النواشر المخروطية المخشنة أن أداؤها يقل بزيادة خشونة السطح كذلك بينت الدراسة أن إمكانية حدوث إنفصال السريان فى النواشر ذات زاوية الإنفراج الكبيرة تقل بزيادة خشونة السطح. فى حالة السريان الدوامى، أوضحت النتائج النظرية أن معدل إضمحلال السريان الدوامى فى النواشر المخروطية يعتمد على درجة خشونة السطح، زاوية الإنفراج، رقم الرينولدز وشدة الدوامات عند المدخل.

أوضحت المقارنة بين النتائج النظرية والمعملية للسريان الإضطرابى الدوامى فى النواشر المخروطية تقاربا معقولا.